Control Management Strategy of Stand-Alone Hybrid Power Micro-System using Super-Capacitor

Randa Kallel*‡, Ghada Boukettaya*, Lotfi Krichen*

*Department of Electrical Engineering, National School of Engineering, University of Sfax, 3038 Sfax, Tunisia

(randa.kallel@hotmail.fr, boukattayaghada@yahoo.fr, lotfi.krichen@enis.rnu.tn)

‡Corresponding Author; Randa Kallel, National School of Engineering 3038 Sfax, Tunisia,
Tel: (216) 74 274 088, Fax: (216) 74 275 595, randa.kallel@hotmail.fr

Received: 10.01.2014 Accepted: 16.02.2014

Abstract- This paper concerns the power management of an isolated hybrid micro-system for residential electricity supply, comprising a variable speed wind turbine (VSWT) and a photovoltaic (PV) panel as principal sources. A super-capacitor (SC) bank is considered as a storage system. These sources are connected to a three-phase load via a unidirectional inverter and an RLC filter. Taking into account the fluctuating nature of renewable sources and the variation of the required power, a diesel engine which is considered as a backup source and a dump load which is regarded as an auxiliary load, are connected on the AC side to ensure balance between the generated and the requested powers. In fact, a control strategy is developed to manage the power flows between the hybrid system devices and to make decision to choose the optimal operating mode ensuring the continuous supply of the load and maintaining the SC state of charge (SOC) at acceptable levels. Simulation results are presented to show the effectiveness of the proposed control system under six operating modes.

Keywords Photovoltaic, Wind, Super-capacitor, Diesel engine, Micro-system, Standalone mode, Control strategy, Power management.

1. Introduction

Energy and environmental problems are the most international concerns today. On the one hand, excessive consumption of fossil fuels threatens the energy reserves of our future generation. On the other hand, it causes a huge quantity of CO2 gas which is the most cause of global warming [1]. Therefore, the interest was to search another source for producing electricity. It seems that renewable energy sources are one of the most reliable and efficient solutions for sustainable and proper energy [1,4]. Nowadays, wind and photovoltaic sources are the most commonly used energy sources all over the world [5- 7]. In some remote regions, where the electrical network connection is impossible or expensive, an autonomous hybrid system is the most attractive solutions for these electrical problems. It is proved that an isolated hybrid system gives a higher efficiency with a low cost, compared to the system with a single source, by the mixture of various renewable sources and different converters [8,9-12]. So, many authors proposed many methods to control the duty cycles of the DC / DC converters which extract the maximum power from the renewable sources and to regulate the DC bus [11]. The most used methods are fuzzy logic, artificial neural network[13, 14] and PI controllers using PWM switches [15]. The weak point of renewable sources is its random production character which is strongly related to fluctuation nature of weather conditions. That's why, it is difficult to implement these sources in an autonomous system without a storage element and very often without a backup source. It is shown that the choice of diesel engine as a backup source for standalone system was considered as the most efficient and economical solution [2]. In this case, several authors elaborated the behavior of autonomous hybrid energy system. They make different combinations of renewable sources (PV-wind turbine (WT)) with storage systems (battery-SC-flywheel-pumped hydro energy storage) and backup power sources (diesel-fuel cell). Therefore, they proposed various power management strategies to control these systems taking into account the variation of weather conditions and required power [12, 16], the most used strategies are fuzzy logic and neuronal networks [17, 18].

The storage systems control is the subject of much research such as reference [19] which compares two methods

Nomenclature

V_w	wind speed (m/s)	R_{sc}	SC resistance(Ω)
β	Pitch angle (°)	C_{sc}	SC capacitor (F)
λ	tip speed ratio	U_{SC}	SC voltage (V)
λ_{opt}	optimum value of the tip speed ratio	U_{mSC}	SC modulated voltage (V)
C_p	power coefficient	SOC	State of charge of the SC
$C_{p\max}$	maximum value of the power coefficient	C_{dc}	DC bus capacitor (F)
ρ	air density (1.22 kg m_3)	U_{dc}	DC bus voltage (V)
R	blade radius (m)	R_t	filter resistance (Ω)
Ω	rotational speed (rad/s)	L_t	filter inductance (H)
R_S	stator winding resistance (Ω)	C_t	filter capacitance (F)
L_S	stator winding inductance (H)	i_{td}, i_{tq}	d and q filter currents (A)
p	number of pole pairs	i_t	filter current (A)
V_{wd}, V_{wq}	d and q components of the stator voltages (V)	i_s	Current in the AC bus (A)
i_{wd}, i_{wq}	d and q components of the stator currents (A)	U_{c1}, U_{c2}	line-to-line voltages (V)
ϕ_m	permanent magnetic rotor flux (Wb)	U_{m1}, U_{m2}	inverter voltages (V)
f	Friction coefficient	U^*_{md}, U^*_{mq}	d and q regulated voltages (V)
i_{mw}	wind turbine generator current (A)	R_{dL}	dump load resistance (Ω)
i_{pv}	photovoltaic current (A)	L_{dL}	dump load inductance (H)
i_{cpv}	current in the photovoltaic capacitor (A)	i_{dL}	dump load current (A)
i_{Lpv}	current in the photovoltaic inductance (A)	K_1	dump load switch
U_{Lpv}	Voltage across the photovoltaic inductance (V)	i_d	diesel current (A)
U_{pv}	Photovoltaic voltage (V)	Ω_d	rotational speed of the diesel engine (rad/s)
U_{mpv}	Photovoltaic modulated voltage (V)	K_2	fuel switch
i_{mpv}	photovoltaic modulated current (A)	K_3	diesel switch
i_{minv}	inverter input current (A)	R_L	load resistance (Ω)
i_{SC}	super-capacitor current (A)	L_L	load inductance (H)
i_{mSC}	super-capacitor modulated current (A)	i_L	load current (A)
L_{sc}	SC inductance (H)	V_c	load voltage (V)

(PI control, sliding mode) to control the DC / DC converter of the SC in a hybrid storage system and shows that the sliding mode presents greater robustness. Reference [9] describes an isolated PV/WT/battery/diesel hybrid system, where, the battery can be charged from the diesel engine, so the inverter acts as a rectifier. Authors in reference [20] describe a hybrid energy storage system (battery and hydrogen system) in photovoltaic energy system operating in stand-alone mode. But this unit presents a problem when the sum of the generated power (by photovoltaic source, battery system and hydrogen system) is lower than the one required by the load. Reference [21] compares four supervisor strategies to control the storage and/or dissipation system to maintain the DC bus constant in DC power distribution system according to two criteria: the voltage performance and efficiency.

In this work, the model and the control of the hybrid micro system devices were developed for Tunisian country. In the beginning, the model of a horizontal axis VSWT driving a permanent magnet synchronous generator (PMSG) is presented. A vector control of this generator has been established to extract the maximum power (MPPT) of the turbine. The generated power is transmitted to the DC bus via a PWM rectifier. Besides, the model PV generator connected to the DC bus through a boost chopper is developed. The DC-DC converter ensures the maximum power of the PV generator using the P&O algorithm [22]. In order to regulate the DC bus, an SC module is associated to the intermittent sources to absorb or supply the power difference, for that it is linked to a buck boost converter in order to control the exchange when SOC limits are respected. These sources supply a three- phase balanced load via a unidirectional inverter and an RLC filter. A diesel engine, turned at a fixed speed, is considered as a backup source and a dump load is considered as an auxiliary load. Both are connected to the AC bus to compensate the variation of production and consumption powers in all operating modes. A Phase Locked Loop (PLL) ensures the synchronization between the different sources established in the hybrid unit.

Finally, for each simulation time, according to weather variable values (irradiation, temperature and wind speed), load energy consumption and SC state of charge, the supervisor strategy takes the decision to choose which the functional component is and what the amount of energy absorbed and/or supplied by the SC is, the diesel engine and the dump load, to achieve two purposes: the continuous supply of the load and the maintaining of the SC state of charge at acceptable level. The obtained simulation results are presented and discussed and the control strategy is validated under different scenarios.

2. Description of the hybrid unit

For small hybrid systems having power below 100 kW, two connection modes (AC bus and DC bus) are widespread [23]. In this context, the studied system connects renewable sources and storage system to the DC bus. In the AC side, the main load, the dump load and the diesel generator are connected to the system through an inverter. And in order to eliminate the harmonics generated by this latter and to get a sinusoidal voltage at its terminals, an RLC filter should be inserted between the inverter and the load, as shown in "Fig.1".

The unit-sizing procedure was established to justify the size of the stand-alone hybrid power micro system components with the proposed structure for residential electricity supply. "Figure 2" depicts the evolution of hourly average required load that shows the specific values: the maximum load power $P_{L\max}$, the minimum load power $P_{L\min}$ which is assumed equal to the permanent and priority load power value.

The hybrid system is designed to supply power to two homes. According to the studied site and standards applied, a 4 kW wind turbine and a 1 kW photovoltaic panel are assumed to be available for this hybrid power micro system. The following unit sizing process is used to determine the size of the SC and the diesel engine. Our objective in this sizing procedure is to reduce the gap $\Delta\overline{P}$ between $\overline{P}_{RE}$ and $\overline{P}_{L}$ such that:

$$\Delta\overline{P} = \overline{P}_{RE} - \overline{P}_{L} \tag{1}$$

Where $\overline{P}_{RE}$ is the average renewable power and $\overline{P}_{L}$ is the average load power estimated at 3.1 kW.

In order to not oversize our system and to ensure technical economic objective, the SC is sized to store the maximum generated renewable power $P_{RE\max}$ when the required power is minimum. Thus, the size of the SC is 2 kW according to the following equation:

$$P_{sc,rated} = P_{RE\max} - P_{L\min} \tag{2}$$

Where $P_{L\min} = P_{L,priority}$ = 2 kW.

The diesel engine is sized to supply priority loads $P_{L,priority}$ where the renewable power is missing (P_{RE} = 0) and the SC is fully discharged (SOC=SOC_{min}). So, the size of the diesel generator is 2 kW according to the following equation:

$$P_{d,rated} = P_{L,priority} \tag{3}$$

2.1. Model and control of the wind system

The aerodynamic power generated by the wind turbine rotor can be written as follows [3, 24]:

$$P_w = \frac{1}{2} C_p(\lambda,\beta)\,\rho\,\pi\,R^2\,V_w^{\,3} \tag{4}$$

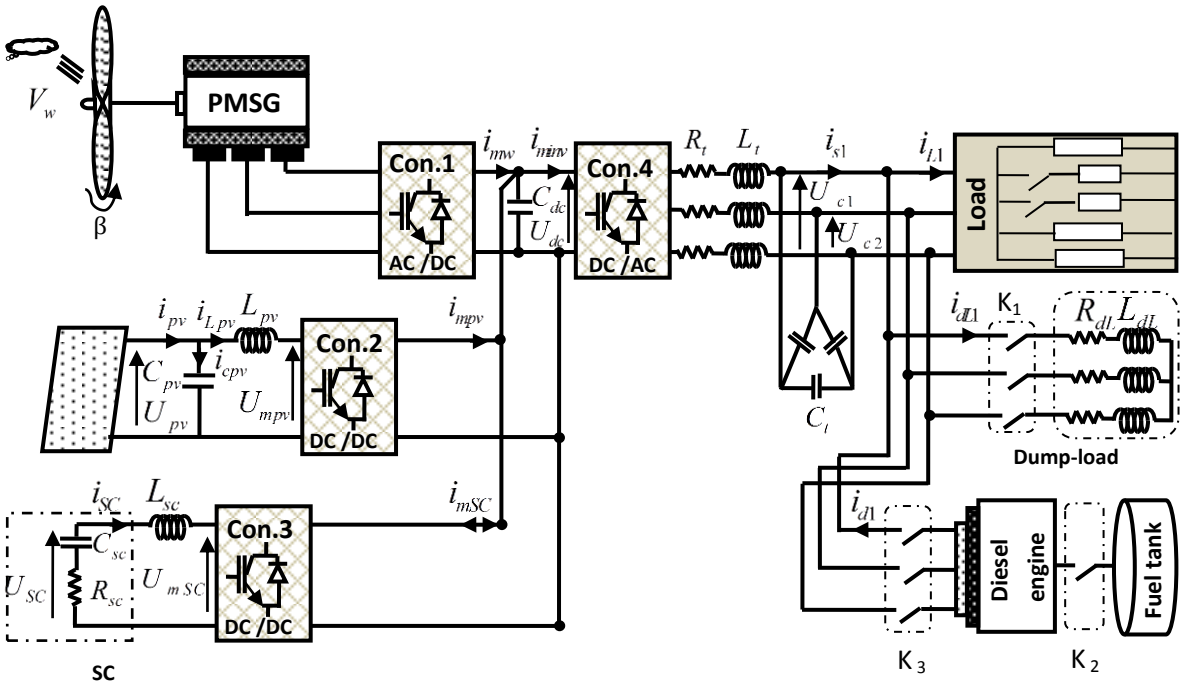

Fig. 1. Architecture of the studied system.

Where ρ is the air density (Kg/m3), R is the radius of the rotor of the VSWT (m) and V_w is the wind speed (m/s).

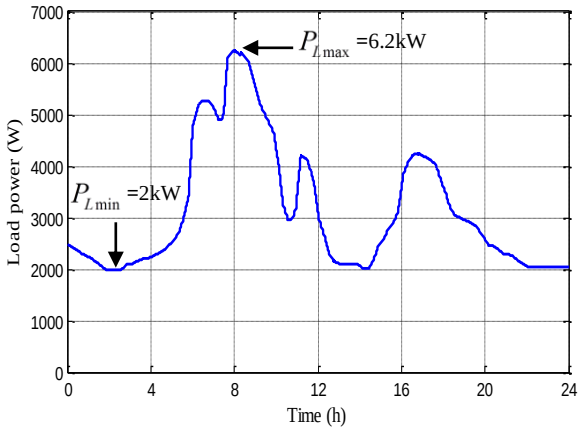

Fig. 2. Hourly average demand of two typical homes

The power coefficient C_p depends on the tip speed ratio λ which is the ratio between the peripheral speed of the blades, the wind speed and the pitch angle β (°) .It is given by the next expression [25]:

$$C_p(\lambda,\beta)=0.53\left(\frac{151}{\lambda_i}-0.53\beta-0.002\beta^{2.14}-13.2\right)\exp\left(\frac{-18.4}{\lambda_i}\right) \quad (5)$$

Where:

$$\lambda_i=\frac{1}{\frac{1}{\lambda-0.02\beta}-\frac{0.003}{\beta^3+1}} \quad (6)$$

$$\lambda=\frac{R\Omega}{V} \quad (7)$$

The electromagnetic torque T_{em} applied to the wind turbine shaft is given by the fundamental equation as follows:

$$J\frac{d\Omega}{dt}=T_m-T_{em}-f\,\Omega \quad (8)$$

Where Ω is the rotational shaft speed of the VSWT (rad/s) and T_m is the turbine torque (Nm) defined by:

$$T_m = \frac{P_w}{\Omega} \tag{9}$$

The model of the MSAP in the Park reference frame is given by the following equations [3, 4]:

$$V_{wd} = R_s i_{wd} + L_s \frac{di_{wd}}{dt} - p\Omega L_s i_{wq} \tag{10}$$

$$V_{wq} = R_s i_{wq} + L_s \frac{di_{wq}}{dt} + p\Omega L_s i_{wd} + p\Omega \phi_m \tag{11}$$

To extract the wind turbine maximum power, the tip speed ratio should be kept to an optimum value λ_{opt} for all wind speeds values. The vector control of the PMSG must maintain i_{sd} equal to zero and adjust the torque by the quadrature current i_{sq}. The stator current i^*_{sq} is calculated from the MPPT block which sets the torque reference T^*_{em} to operate at maximum power point tracking (MPPT) as shown in control conv. 1 section A in "Fig.3". It's expressed by:

$$i^*_{sq} = \frac{T^*_{em}}{p\phi_m} \tag{12}$$

2.2. Model and Control of the PV System

The photovoltaic generator converts the solar energy into electrical energy through photovoltaic cells connected in series or/and in parallel to obtain the desired value of the voltage and current at the output of photovoltaic panel (PV) [9, 26]. The solar power as a function of solar irradiation E can be predicted by the equation given below:

$$P_{pv} = aE^2 + bE + c \tag{13}$$

a, b and c are constants that can be obtained from measured data.

The photovoltaic power increases when the irradiation increases and decreases when the temperature increases [7].

The duty cycle α_{pv} of the DC/DC photovoltaic converter is calculated from the reference voltage U^*_{pv} provided by the MPPT and two PI regulators as shown in control conv. 2 section A in "Fig.3". These PI regulators are defined by the following equations:

$$U^*_{Lpv} = PI\,(i^*_{Lpv} - i_{Lpv}) \tag{14}$$

$$i^*_{cpv} = PI\,(U^*_{pv} - U_{pv}) \tag{15}$$

2.3. Model and control of the SC storage system

The power management requires a storage system which has a high dynamic response to compensate the difference between generated and required powers. The SC storage system appears to be the solution because it presents an evolution in its dynamic performance, reduced manufacturing costs and more time service life compared to other storage systems [27].

The model of SC comprises a capacitor C_t, an equivalent series resistor ESR representing the charging and discharging resistor and an equivalent parallel resistor ERP representing the loss of self-discharging. The energy quantity drawn from the super-capacitor bank is proportional to the capacitor C_t and the square of the voltage variation [28]. This energy E_{SC} can be positive or negative depending on the super-capacitor state (discharge / charge) according to the following equation:

$$E_{SC} = \frac{1}{2} C_t (V_i^2 - V_f^2) \tag{16}$$

Where V_i and V_f represent the initial and the final voltage of the super-capacitor.

The total resistor and the total capacitor of the bank are given by the following expressions [28]:

$$R_{sc-total} = n_S \frac{ESR}{n_P} \tag{17}$$

$$C_{sc-total} = n_P \frac{C_t}{n_S} \tag{18}$$

Where n_s and n_p are the number of super-capacitor units placed respectively in series and in parallel.

The aim of the SC control is to set the i_{SC} current to its reference value i^*_{SC}. This reference current is imposed by the control algorithm of the hybrid system. So a current loop is developed to regulate the SC current using a PI regulator as shown in control conv. 3 section A in "Fig.3". This current is given by the following differential equation:

$$L_{sc} \frac{di_{SC}}{dt} = U_{SC} - U_{mSC} \tag{19}$$

The power exchanged by the SC is given by:

$$P_{SC} = i_{mSC} U_{dc} \tag{20}$$

The management of the SC power ensures the control of the DC bus voltage which is maintained constant. The DC bus control loop is represented in control DC bus section A in "Fig.3".

The DC bus current i_{dc} depends on the current flow management as follows:

$$i_{dc} = i_{mw} + i_{mpv} + i_{msc} - i_{minv} \tag{21}$$

2.4. Control of the Inverter

The control signals of the DC/AC converter are generated from two resonant regulators which control the voltages across the load U_{c1} and U_{c2} using the transfer function of the RLC filter, as shown in control conv. 4 section A in "Fig.3". This transfer function connects the composed voltages U_{c1}, U_{c2} to the modulated voltages U_{m1}, U_{m2} which are measured at the inverter output as follows:

$$\frac{U_{c1}}{U_{m1}} = \frac{U_{c2}}{U_{m2}} = \frac{1}{1 + 3R_t C_t s + 3L_t C_t s^2} \tag{22}$$

The transfer function of the resonant regulator is expressed by [29]:

$$C(s) = \frac{c_0 + c_1 s + c_2 s^2 + c_3 s^3}{\left(d_0 + d_1 s\right)\left(s^2 + w_p{}^2\right)} \tag{23}$$

c_0, c_1, c_2, c_3, d_0 and d_1 are the parameters of the resonant correction and w_p is the pulse of the reference voltages.

The current and the voltages across the RLC filter are given as follows:

$$\frac{d}{dt}\begin{pmatrix} i_{t1} \\ i_{t2} \end{pmatrix} = \frac{-R_t}{L_t}\begin{pmatrix} 1 & 0 \\ 0 & 1 \end{pmatrix}\begin{pmatrix} i_{t1} \\ i_{t2} \end{pmatrix} + \frac{1}{3L_t}\begin{pmatrix} 2 & -1 \\ -1 & 2 \end{pmatrix}\begin{pmatrix} U_{m1} - U_{c1} \\ U_{m2} - U_{c2} \end{pmatrix} \tag{24}$$

$$\frac{d}{dt}\begin{pmatrix} U_{c1} \\ U_{c2} \end{pmatrix} = \frac{1}{3C_t}\begin{pmatrix} 2 & 1 \\ 1 & 2 \end{pmatrix}\begin{pmatrix} i_{t1} - i_{s1} \\ i_{t2} - i_{s2} \end{pmatrix} \tag{25}$$

The modulated inverter current $i_{\min v}$ is given by the following equation:

$$i_{minv} = \frac{1}{2}\left(U^*{}_{md} i_{td} + U^*{}_{mq} i_{tq}\right) \tag{26}$$

The AC bus resulted current i_s is given by the following equation:

$$[i_s]_{1,2,3} = [i_L]_{1,2,3} + [i_{dL}]_{1,2,3} - [i_d]_{1,2,3} \tag{27}$$

As shown in section B figure 3, and according to the SC power and its state of charge, the supervisor determines the reference power values of each device connected to the AC bus: the dump load reference power $P^*{}_{dL}$, the load reference power $\bar{P}^*_L$ and the diesel fuel consumption control. The supervisor decides the on or the off times of the switches K_1 and K_2.

2.5. Model of the Diesel Generator

The diesel generator is currently used in several applications [30]. It is used to cover the needs of peak consumption and especially for the electricity supply in isolated sites, in particular in emergency cases. This generator is composed of a diesel engine associated with a synchronous generator.

A simplified model of the diesel generator is comprised by a first order actuator linked to a time delay which represents the fuel combustion delay τ_c and the ignition retard τ_d. If we consider F as the fuel level gain, the torque T_d associated to the diesel generator is expressed as follows [26]:

$$T_d = \frac{F}{1 + \tau_c s} e^{-\tau_d s} \tag{28}$$

When the supervisor takes the decision to close the switch K_2, the rotational speed Ω_d of the considered diesel generator begins to grow (starting engine) until it reaches its nominal value Ω_{dn} after one minute. In this moment, the switch K_3 will be closed to ensure that the diesel generator operates at its rated power $P^*{}_d$.

2.6. Model of the load

In this study, the hybrid unit is used to supply a three-phase isolated load. Its characteristics are given by the following equations:

$$R_L = \frac{V_c{}^2 P^*{}_L}{P^*{}_L{}^2 + Q^*{}_L{}^2} \tag{29}$$

$$L_L = \frac{V_c{}^2 Q^*{}_L}{P^*{}_L{}^2 + Q^*{}_L{}^2} \tag{30}$$

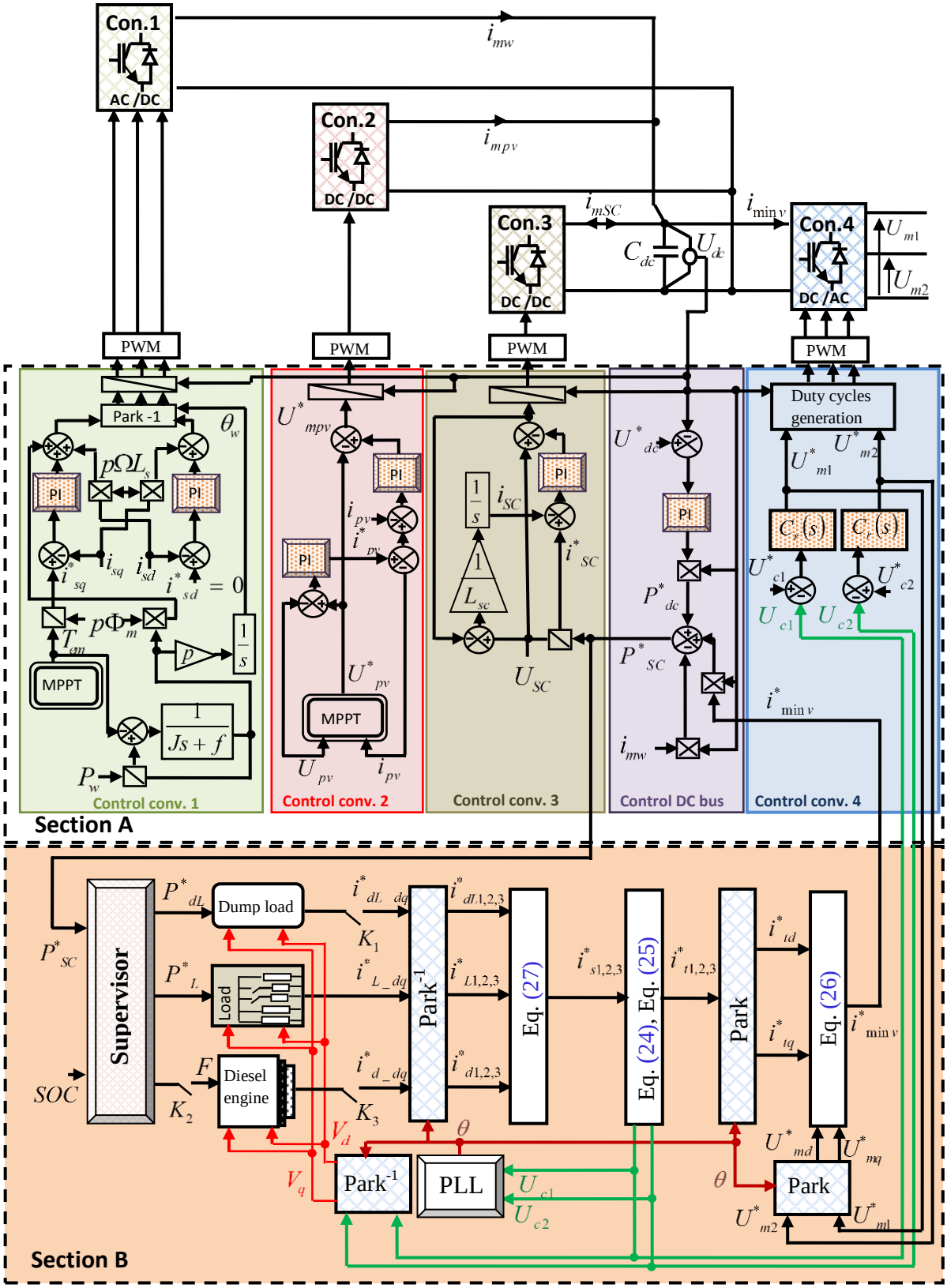

Fig. 3. Control scheme of the hybrid system.

Where V_c is is the simple voltage across the RLC filter.

The loads are supplied by priority. In critical cases, which are well explained in the control algorithm, the required load power can be decreased by the elimination of non-priority load.

2.7. Model of the Dump Load

Usually, in the case of a surplus power in an isolated hybrid unit, the wind power should be reduced by acting on the pitch angle β or by operating the photovoltaic generator without MPPT control. In this study, the degraded power is used to supply water pumping system as a dump load especially for domestic applications. So, this power is not lost. Therefore, apart from the load, a hybrid may also contain auxiliary loads to achieve energy balance. The dump load currents in dq frame $i_{dL,d}$, $i_{dL,q}$ are calculated from the reference power P^*_{dL} set by the management algorithm as follows:

$$i_{dL\_d} = \frac{P^*_{dL} V_d + Q^*_{dL} V_q}{V_d^{\,2} + V_q^{\,2}} \tag{31}$$

$$i_{dL\_q} = \frac{P^*_{dL} V_q - Q^*_{dL} V_d}{V_d^{\,2} + V_q^{\,2}} \tag{32}$$

Where V_d and V_q are the composed voltages U_{c1} and U_{c2} in dq frame, respectively.

The reactive power is calculated from the active power:

$$Q^*_{dL} = P^*_{dL} tg(\varphi) \tag{33}$$

Where φ is the phase angle between the current and the voltage at the terminal of the RLC filter.

3. Power Management Supervisor

The purpose of the proposed system is to supply small sites of houses with predicted power consumption around an average of 3.1 kW and a water pumping system as an auxiliary load. A power management supervisor is designed for hybrid solar-wind-diesel power system, to guarantee the required load power under various weather conditions. In this case, the SC has been used as an energy buffer in the hybrid system, i.e. maintaining constant the bus voltage following any change of the transited power [26]. Therefore, during its operation, the SC can undergo: overcharging for exceeding its SOC at 90% and deep discharge for a decrease of the SOC above 30%. In the case where the load is sufficiently supplied and the SC is fully charged, the integration of a dump load as an auxiliary load is necessary to dissipate the surplus power. And in the case where the generated power is not enough to supply the load and the SC is completely discharged, the implantation of diesel generator is the optimal solution to compensate the energy deficit. Thus, we propose an algorithm to manage the power flow in the hybrid autonomous system under various conditions: wind speed, irradiation and temperature fluctuation, load power consumption and SOC level. This algorithm is based on several constraints which are:

- Continuous supplying of the load.
- Using in priority the SC as storage/backup system when the diesel generator and the dump load operate in the last case, ensuring a balance between generated and consumed powers. Thus, the power balance equation can be written as follow:

$$P_{SC} = P_{dL} + P_L - P_{RE} - P_d \tag{34}$$

- Charging the super-capacitor only from renewable sources.
- Minimizing the diesel generator operation.
- Preventing SC deep discharge (SOC>SOC_{min}) and SC overcharge (SOC<=SOC_{max}).

This study is carried out to ensure the system autonomy and to meet the established energy constraints. Then, the developed algorithm associated to the power management supervisor requires the knowledge of produced and consumed powers and the SC state of charge, to control the dump load reference power, operating diesel power and the reference load power consumption, according to six operating modes as shown in "Fig.4". In addition to these references, the buck boost converter controls the exchanged power by the SC to regulate the DC bus voltage.

- SC charge power mode (**mode 1**): in this case, according to the system power balance, the SC power is negative i.e. the generated renewable power is greater than the required power ($P_{RE} > P_L$). The excess power must be stored in the SC module while the maximum state of charge level is not reached. Therefore, the diesel power and dump load power, both are equal to zero.
- SC discharge power mode (**mode 2**): in this case, according to the system power balance, the SC power is positive i.e. the generated power is not enough to supply the load ($P_{RE} < P_L$). Thus, the SC must cover the missing power when the SOC does not achieve its minimum value SOC_{min}=0.3. So, neither the diesel engine nor the dump load is operated.

Two modes appear when the SC state of charge reaches its minimum or maximum level: the diesel engine operating mode and the dump load operating mode.

- Diesel engine operating mode: in this case, there is an under production and the SC is fully discharged (SOC=SOC_{min} and P^*_{SC} =0). Thus, the K_2 switch is turned

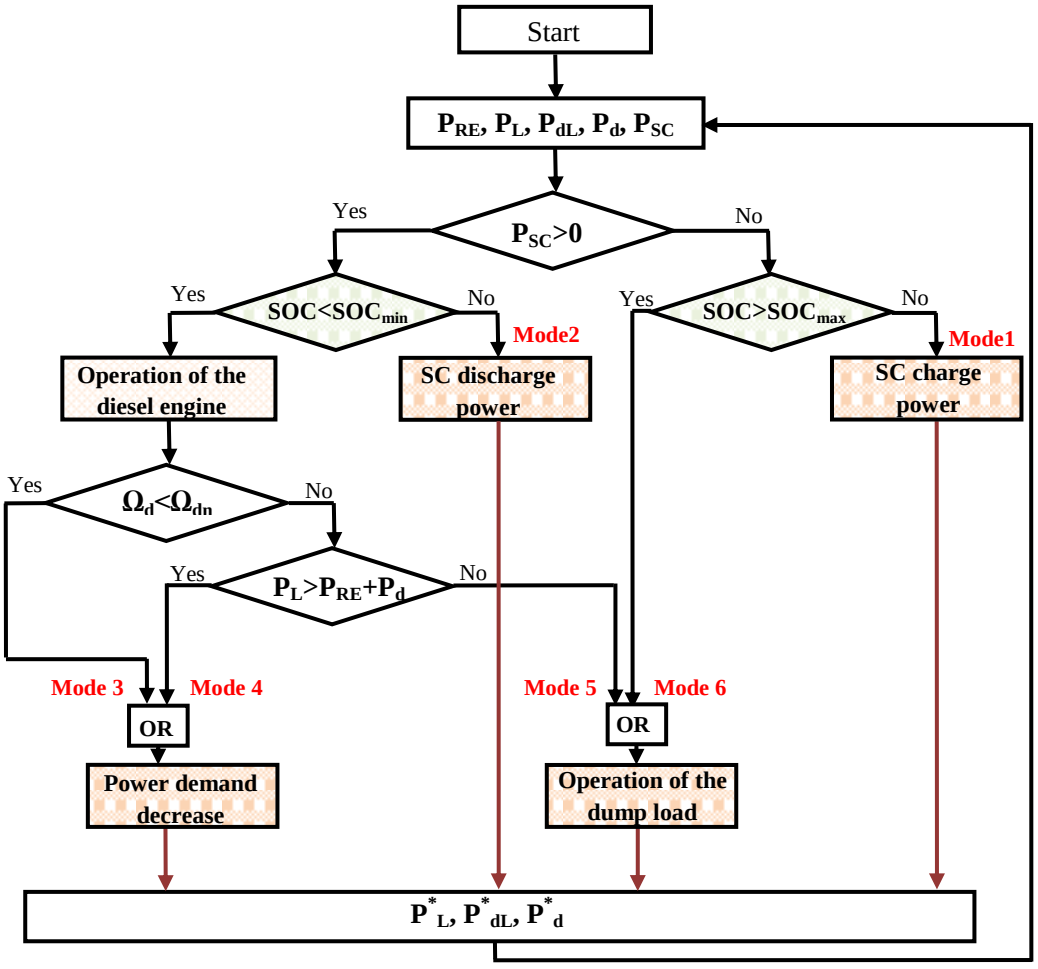

Fig. 4. Power management system algorithm.

on ensuring the diesel engine starting. This latter must reach a certain rotational speed Ω_{dn} to be able to operate in its nominal power. According to the diesel rotational speed, two new modes will appear that will be explained later.

➢ Power demand decrease mode: in this case, the rotational speed is less than its nominal value: $\Omega_d < \Omega_{dn}$ (**mode 3**). Under this condition, there is not diesel power production, the non priority loads are turned off. So, the power sent to the load is $P^*_L = P_{RE}$ and P^*_{dL}=0. Otherwise, when the rotational speed reaches its nominal value after one minute $\Omega_d = \Omega_{dn}$ (**mode 4**), the K_3 switch is turned on and the diesel engine operates at its rated power P^*_d = 2kW. However, if there is a high load power peak, the generated power is not enough to supply the load ($(P_{RE} + P^*_d) < P_L$), the required power will be decreased by eliminating the non priority loads. The reference load power is $P^*_L = P_{RE} + P^*_d$ and the dump load power is equal to zero.

➢ Dump load operating mode: the dump load can be supplied by the diesel engine when $\Omega_d = \Omega_{dn}$ and $(P_{RE} + P^*_d) > P_L$ (**mode 5**). So, the difference power must be sent to the dump load $P^*_{dL} = P_{RE} + P^*_d - P_L$. Also, it can be supplied by the renewable sources when there is an over production $P_{RE} > P_L$ and the SC is fully charged SOC=SOC_{max}=0.9(**mode 6**). Thus, $P^*_{SC} = 0$, and $P^*_{dL} = P_{RE} - P_L$.

4. Simulation Results and Discussion

The hybrid energy system model and the developed control strategy are implemented in MATLAB/Simulink software using the studied system parameters illustrated in "Table 1". In order to validate the proposed control management strategy and the convergence of the adopted algorithm, the system is simulated according to the weather variable conditions and to the required power level that are given by "Fig.5" during 450s.

The wind and the photovoltaic generators are the principal energy sources in the studied hybrid system. Then, the wind turbine is controlled by the pitch control, and the photovoltaic generator is controlled by the MPPT controller.

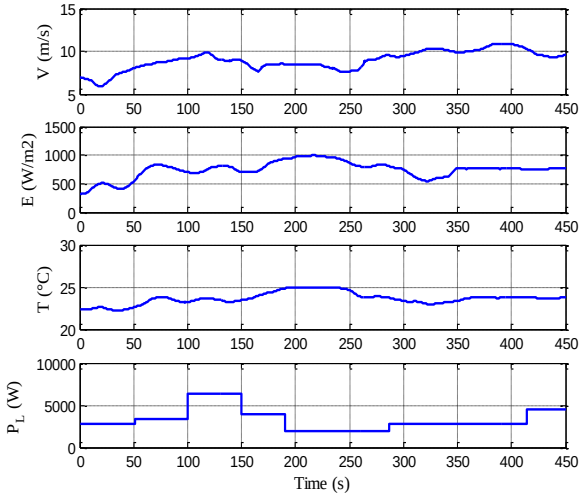

Fig. 5. Simulation constraints.

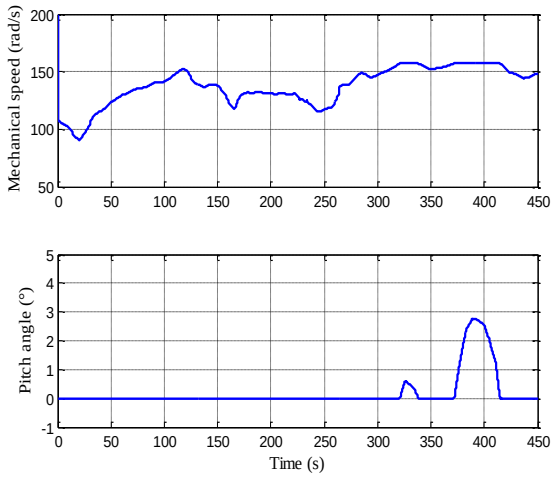

Fig. 6. Mechanical speed and pitch angle of the wind

To ensure the wind turbine protection, a mechanical device "Pitch Control" is developed to limit the turbine rotational speed. This mechanism is available to control the blades angle at a reference angle β^* when the wind speed reaches its rated value V_{wr} =10.2 m/s as shown in "Fig.6".

Therefore, this control system operation reduces the power coefficient C_p and decreases the speed ratio λ as shown in "Fig.7".

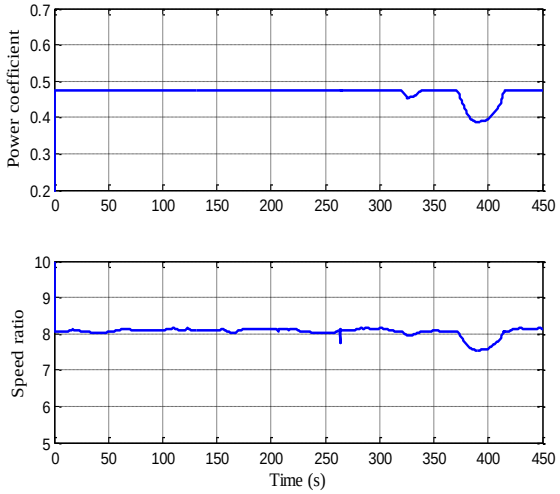

Fig. 7. Power coefficient and speed ratio.

"Figure 8" shows the different power of the hybrid system devices. This figure proves the effectiveness of the developed control management supervisor according to the profiles of the six operating modes which are presented in "Fig.9".

Between the intervals [0, 58.5 s] and [415, 450 s], the hybrid unit operates in mode 2: the discharge mode. The generated renewable power is less than the required power. So, the SC must cover the missing power in order to satisfy the load $P^*_{SC} = -\left(P_{RE} - P_L\right)$ when the SOC does not achieve its minimum value. During the interval [58.5, 118.5s], mode 3 is activated, the SOC reaches its minimum value as shown in "Fig.10".

Therefore, the intervention of the diesel engine as a backup source is necessary. During its starting time, the diesel rotational speed Ω_d begins to grow exponentially to achieve after one minute its nominal value.

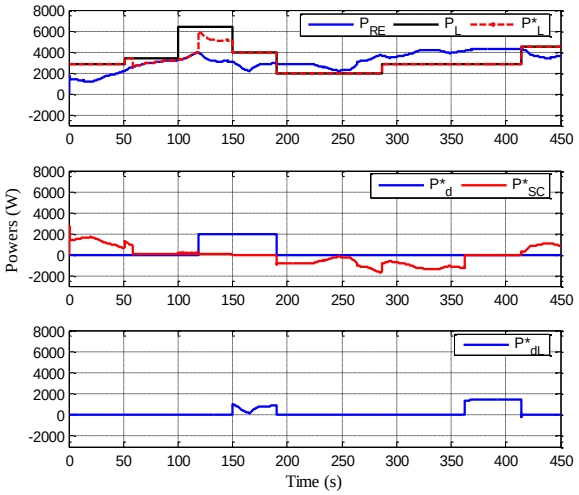

Fig. 8. Power assessment.

In this gap of time, the switch K_3 is turned off and consequently the diesel current is equal to zero. The power correction is made by eliminating the non-priority load. So, $P^*_{SC} = 0$, $P^*_d = 0$ and $\overline{P}^*_L = P_{RE}$.

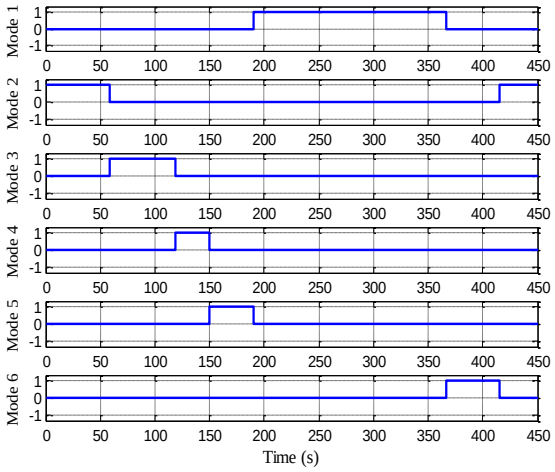

Fig. 9. Different operating modes.

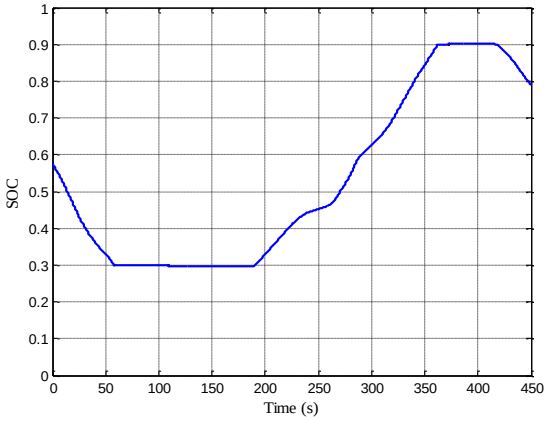

Fig. 10. State of charge of the SC.

When the diesel speed reaches its nominal as shown in "Fig.11", two modes will appear: mode 4 and mode 5. In the interval [118.5, 150 s], mode 4 is activated, we observe a high peak load power demand, in fact $\left(P_{RE} + P^*_d\right) < P_L$. The required power must be decreased. So, $P^*_{SC} = 0$, $P^*_d = 2kW$ and $P^*_L = P_{RE} + P^*_d$. During the interval [150, 190 s], the hybrid system operates in mode 5, there is an excess power $(P_{RE} + P^*_d) > P_L$. The existing solution to balance the system is supplying the dump load. So, $P^*_{SC} = 0$, $P^*_d = 2kW$, $P^*_L = P_L$ and $P^*_{dL} = P_{RE} + P^*_d - P_L$.

In the interval [190, 367 s], the hybrid unit operates in mode 1: the recovery mode. The generated power is greater than the required power. The SC must store the excess power while the maximum SOC level is not reached. So, the power forwarded to the SC is the difference power $P^*_{SC} = -(P_{RE} - P_L)$. During the interval [367, 415 s], mode 6 is activated when the SOC achieves its maximum value. So, the SC is fully charged. Therefore, the excess power is sent to supply the dump load. Thus, $P^*_{SC} = 0$, and $P^*_{dL} = P_{RE} - P_L$.

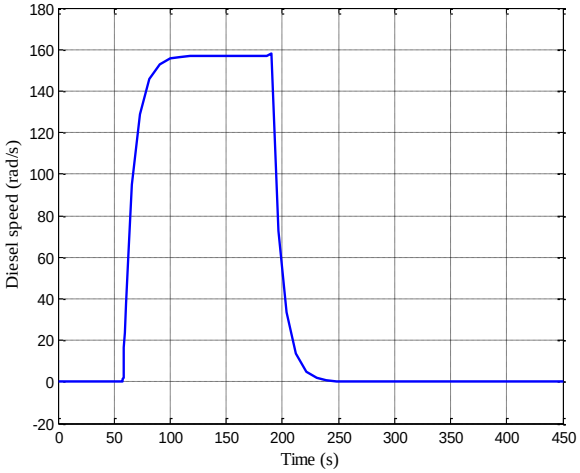

Fig. 11. Diesel rotational speed .

The power balance between the different hybrid system devices enables the adjustment of the DC bus voltage and maintaining it at its reference value $U^*_{dc} = 700V$ is shown in "Fig.12". This figure shows the effectiveness of the elaborated control strategy.

"Figure 13", "Figure 14", "Figure 15", and"Figure 16", show the load reference current i^*_L, the dump load reference current i^*_{dL}, the diesel reference current i^*_d and the resulting current in the AC bus i^*_s, respectively. The zooms applied for each current prove the effectiveness of the implemented PLL control ensuring the synchronization between the hybrid system devices.

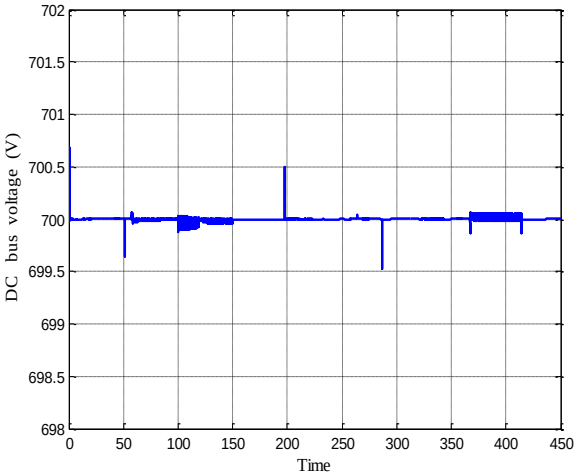

Fig. 12. DC bus voltage.

"Figure 17", "Figure 18" and "Figure 19" show respectively: the two voltages at the RLC filter output U_{c1} and U_{c2} with the associated references U^*_{c1} and U^*_{c2}, the voltage V_{c1} and the current i_{L1} at the first phase of the load and the regulated voltages across the load U^*_{m1} and U^*_{m2}. These figures validate the load control system and the zoom during 0.08 s on each figure shows the stability of the system control during load variation.

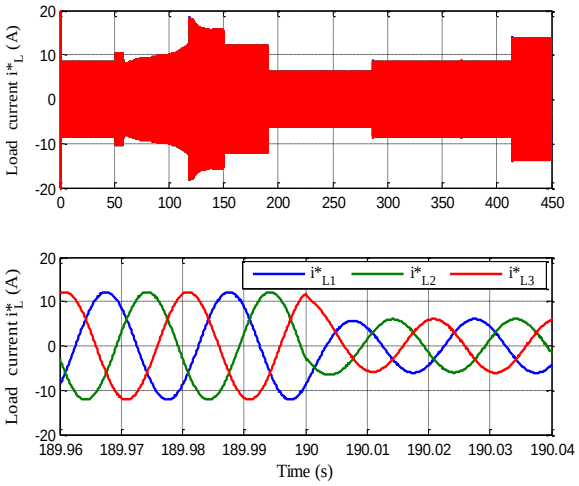

Fig. 13. Load current.

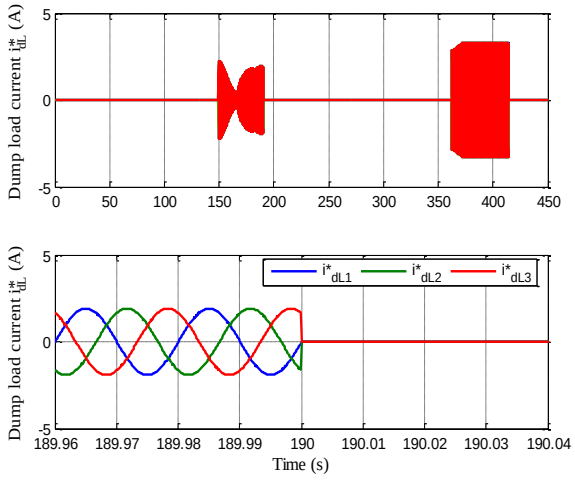

Fig. 14. Dump load current.

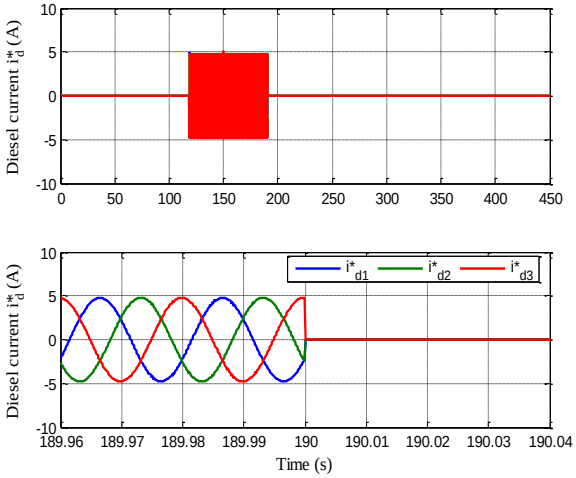

Fig. 15. Diesel current.

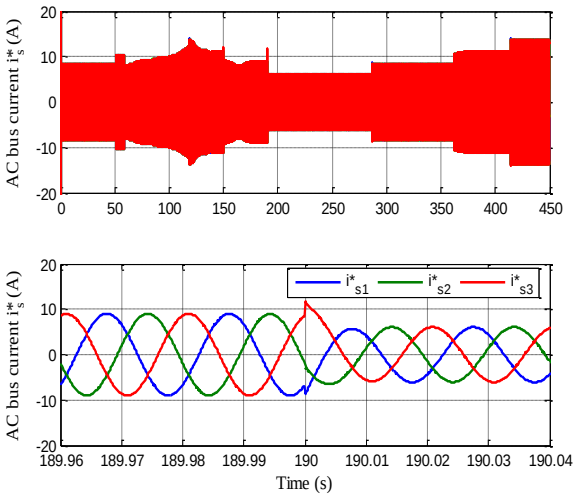

Fig. 16. AC bus current.

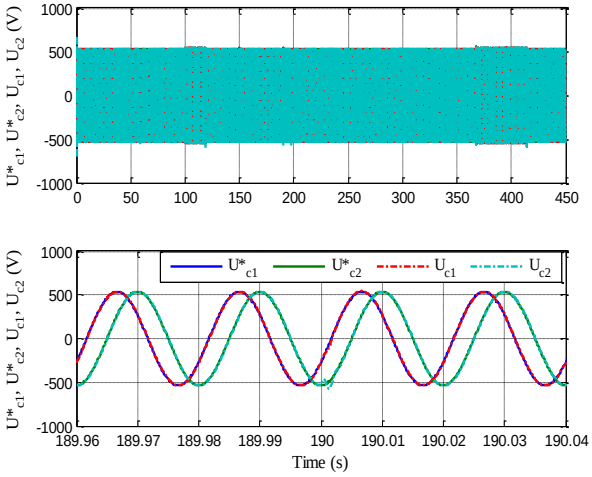

Fig. 17. Voltages at the RLC filter output and its references.

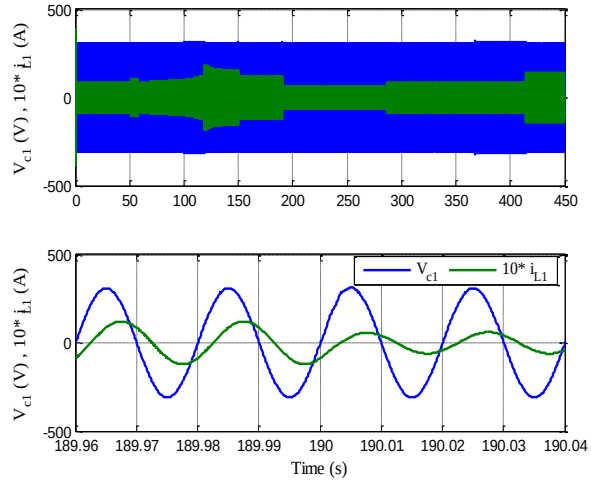

Fig. 18. Voltage and current of the load first phase ($\cos\varphi$ =45°).

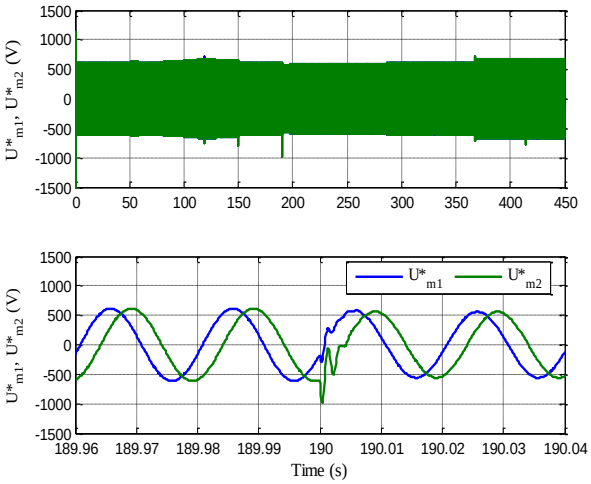

Fig. 19. Reference voltages across the load.

5. Conclusion

This paper presented an optimal control management strategy of an autonomous (VSWT/PV/SC/diesel) unit supplying a small site comprising several houses as a main load and a water pumping system as an auxiliary load. The diesel engine is operated as a backup source by supplying load in the emergency cases. A supervision strategy is developed to manage power flows between the different energy sources and the SC storage system. Then, the supervisor makes decision to choose the operating mode in order to guarantee the continuous supply of the load and maintain the state of charge of the SC at an acceptable level. Simulation results show the effectiveness of this management strategy depending on the weather conditions and the required load variation using a six-mode operating algorithm.

Table 1. Studied system parameters.

Wind turbine	Number of blades	3
PMSG	Blade radius	2
	Nominal power	3.850 kW
	Number of pole pairs	4
	Stator winding resistance	0.82Ω
	Stator winding inductance	15.1mH
	Permanent magnetic rotor flux	0.45 Wb
	Inertia	99.10^{-4} Kg m^2
	Friction coefficient	10^{-3} N m s rad^{-1}
PV generator	Number of modules in series	15
	Number of modules in parallel	1
	Number of cells in series	36
	Number of cells in parallel	1
	Maximum power / module	130 W
	Open circuit voltage / module	22.1 V
	Short Circuit Current /module	8.06 A
SC [BMOD0094]	Capacitance	94 F + 20-0%
	Rated voltage	75 V
	ESR	12.5 mΩ
	Leakage current	0.15 A, 75 h, 25°C
	Operating temperature	-40°C to +65°C
	Maximum DC current	50 A
DC bus	Capacitance	2200 µF
RLC filter	Filter resistance	0.1 Ω
	Filter inductance	25 mH
	Filter capacitance	9 µF
Diesel generator [DG 2500 L]	Rated power	2 kW
	Maximum power	2.2 kW
	Fuel combustion delay τ_c	0.2 s
	Ignition retard τ_d	0.003s
	Rated rotational speed Ω_{dn}	157 rad/s

References

[1] S. Abedi, A. Alimardani, G. B. Gharehpetian, G .H. Riahy, and S. H. Hosseinian, "A comprehensive method for optimal power management and design of hybrid RES-based autonomous energy systems," *Renewable and Sustainable Energy Reviews*, vol. 16, pp. 1577- 1587, 2012.

[2] S. Diaf, M. Belhamel, M. Haddadi, and A. Louche, "Technical and economic assessment of hybrid photovoltaic/wind system with battery storage in Corsica island," *Energy Policy*, vol. 36, pp. 743-754, 2008.

[3] A. Masmoudi, A. Abdelkafi, and L. Krichen, "Electric power generation based on variable speed wind turbine under load disturbance," *Energy*, vol. 36, pp. 5016-5026, 2011.

[4] A. Abdelkafi, A. Masmoudi, and L. Krichen, "Experimental investigation on the performance of an autonomous wind energy conversion system," *Electrical Power and Energy Systems*, vol. 44, pp. 581-590, 2013.

[5] J.Wen, Y. Zheng, F. Donghan, "A review on reliability assessment for wind power," *Renewable and Sustainable Energy Reviews*, vol. 13, pp. 2485-2494, 2009.

[6] M. Hoogwijk, B. De Vries, W. Turkenburg, "Assessment of the global and regional geographical, technical and economic potential of onshore wind energy," *Energy Economy*, vol. *26*, pp. 889-919, 2004.

[7] C. Wang, M. H. Nehrir, " Power Management of a Stand-Alone Wind/Photovoltaic/Fuel Cell Energy System,"*IEEE transactions on energy conversion*, vol. 23, 2008.

[8] B. Heyrman, A. A. Abdallh, Luc Dupré, " Efficient Modeling, Control and Optimization of Hybrid Renewable-Conventional Energy Systems," *International journal of renewable energy research*, vol. 3, No.4, 2013.

[9] A. K. Daud, and M. S. Ismail, " Design of isolated hybrid systems minimizing costs and pollutant emissions,"*Renewable Energy*, vol. 44, pp. 215-224, 2012.

[10] A. Hajizadeh, and M. A. Golkar, "Intelligent power management strategy of hybrid distributed generation system,"*Electrical Power and Energy Systems*, vol. 29, pp. 783-795, 2007.

[11] P. Nema, R. K. Nema, S. Rangnekar, " A current and future state of art development of hybrid energy system using wind and PV solar – A review," *Renewable and Sustainable Energy Reviews*, vol. 13,pp. 2096-2103, 2009.

[12] J. L. B. Agustın, and R. D. Lopez, "Simulation and optimization of stand-alone hybrid renewable energy systems," *Renewable and Sustainable Energy Reviews*, vol. 13, pp. 2111-2118, 2009.

[13] M. Hattia, A. Meharrarb, M. Tioursic, "Power management strategy in the alternative EPV/PEM fuel cell hybrid system," *Renewable and Sustainable Energy Reviews*, vol. 15, pp. 5104-5110, 2011.

[14] S. B. Skretas, and D. P. Papadopoulos, "Efficient design and simulation of an expandable hybrid (wind/ PV) power system with MPPT and inverter input voltage regulation features in compliance with electric grid requirements," *Electric Power Systems Research*, vol. 79, pp. 1271-1285, 2009.

[15] N. A. Ahmed, and A. K. Al-Othman, "AlRashidi M R. Development of an efficient utility interactive combined wind /PV/fuel cell power system with MPPT and DC bus voltage regulation," *Electric Power Systems Research*, vol. 81, pp. 1096-1106, 2011.

[16] O. C. Onar, M. Uzunoglu, and M. S. Alam, "Modelling control and simulation of an autonomous wind turbine /PV /FC / ultra capacitor hybrid system," *Journal of Power Sources* , vol. 185, pp. 1273-1283, 2008.

[17] O. Erdinc, O. Elma, M. Uzunoglu, U. S. Selamogullari, B. Vural, E. Ugur, A. R. Boynuegri, and S. Dusmez, " Experimental performance assessment of an online energy management strategy for varying renewable power production suppression," *International Journal of Hydrogen Energy*, vol. 37, pp. 4737–4748, 2012.

[18] M. Hatti, and M.Tioursi, "Dynamic neural network controller model of PEM fuel cell system," *International Journal Hydrogen Energy*, vol. 34, pp. 5015-5021, 2009.

[19] A. Etxeberria, I. Vechiu, H. Camblong, and J. M. Vinassa, "Comparison of sliding mode and PI control of hybrid energy system storage in a micro-grid application," *Procedia Energy* , vol. 12, pp. 966 -974, 2011.

[20] C. H. Li, X. J. Zhu, G. Y. Cao, S. Sui, and M. R. Hu, "Dynamics modeling and sizing optimization of stand-alone photovoltaic power systems using hybrid energy storage technology," *Renewable Energy*, vol. 34, pp. 815-826, 2009.

[21] H. Zhang, C. Saudemont, B. Robyns, and R. Meuret, "Comparison of different DC voltage supervision strategies in local power distribution system of more electric aircraft," *Mathematics and Computers in Simulation*, vol. 81, pp. 263-276, 2010.

[22] C. Hua, J. Lin, and C. Shen, "Implementation of a DSP controlled photovoltaic system with peak power tracking," *IEEE Trans. Ind. Elecron*, vol. 45, pp. 99-107, 1998.

[23] O. Carlson, "Wind-hybrid systems with variable speed and DC-link," *Wind Power for the 21 centry*, Kassel. Germany, pp. 25-27, 2000.

[24] A. G. Aissaoui, A. Tahour, N. Essounbouli, F. Nollet, M. Abid, and M. I. Chergui, "A fuzzy –PI control to extract an optimal power from wind turbine," *Energy Conversion and Management*, vol. 65, pp. 688–696, 2013.

[25] W. M. Lin, C. M. Hong, "Intelligent approach to maximum power point tracking control strategy for variable-speed wind turbine generation system," *Energy*, vol. 35, pp. 2440-2447, 2010.

[26] G. Boukettaya, L. Krichen, and A. Ouali, "A comparative study of three different sensorless vector control strategies for a Flywheel Energy Storage System," *Energy*, vol. 35, pp. 132-139, 2010.

[27] Ciu H. Mao, J. Lu, and D.Wang, "Electronic power transformer with supercapacitors storage energy system," *Electric Systems research*, vol. 79, pp. 1200-1208, 2009.

[28] M. Zunoglu. O. Onar, and M. S. Alam, "Modeling, control and simulation of a PV/FC/UC based hybrid power generation system for stand-alone application," *Renewable Energy, vol.* 34, pp. 509–520, 2009.

[29] Ph. Delarue, A. Bouscayrol, and E. Semail, "Generic control method of multi-leg voltage- source-converters for fast practical implementation," *IEEE Trans Power Electron , vol.* 18, pp. 517-526, 2003.

[30] T. Balamurugan, S. Manoharan, " Optimal Power Flow Management Control for Grid Connected Photovoltaic/Wind turbine/Diesel generator (GCPWD) Hybrid System with Batteries," *International journal of renewable energy research*, vol. 3, No.4, 2013.